Available online at website: https://journal.bcrec.id/index.php/bcrec

Bulletin of Chemical Reaction Engineering & Catalysis, 20 (3) 2025, 517-534

Original Research Article

Kinetics Model and Optimization for Photocatalytic Degradation of Methylene Blue over Ag/TiO_2 Catalyst

Amna Jwad Kadem§, Xian Jin Lau§, Swee-Yong Pung, Srimala Sreekantan, Sivakumar Ramakrishnan*

School of Materials and Mineral Resources Engineering, Engineering Campus, Universiti Sains Malaysia, 14300 Nibong Tebal, Penang, Malaysia

Received: 10th June 2025; Revised: 1st August 2025; Accepted: 1st August 2025
Available online: 12th August 2025; Published regularly: October 2025

Abstract

Titanium dioxide (TiO_2) particles are widely used as photocatalysts due to their stability, low toxicity, and relatively low cost. However, their application is limited by a wide bandgap and a high recombination rate. This project investigated the photocatalytic performance of Ag/TiO_2 catalyst, prepared by coupling Ag metal to TiO_2 using the liquid impregnation method. The photocatalytic activity of different concentrations of Ag metal solutions and different pH levels of Ag/TiO_2 catalyst under UV and visible light irradiation was observed. It was shown that Ag/TiO_2 catalyst had the best photodegradation efficiency (83.82%) and the highest rate constant (0.03298 min^{-1}) in 50 ppm Ag metal concentration and at pH 5 under UV light irradiation. The operating conditions were optimised by using the Design of Experiment (DOE) and Response Surface Methodology (RSM) to obtain optimum photodegradation efficiency (PE). The optimum parameters were 22.6263 ppm Ag metal solution and pH of 5, which were estimated to produce the highest photodegradation efficiency (84.0006 %) and rate constant (0.0321 min^{-1}). The concentration of the methylene blue (MB) followed a first-order exponential decay and showed a decreasing trend from its initial concentration. In addition, the photocatalytic degradation rate of MB has been modelled successfully by Power Law kinetic model derived from the Langmuir-Hinshelwood framework. Numerical and analytical methods were implemented to solve the Langmuir-Hinshelwood equation, and both methods were very effective in agreement with the trend shown by the experimental data. In terms of photodegradation efficiency, the kinetic model has slightly over predicted the experimental model due to some minor experimental error, but the experimental data effectively complied with the theoretical micro kinetics investigations simulated using Power Law kinetic model.

Keywords: Photodegradation; Photocatalyst; TiO2; Ag/TiO2; Langmuir-Hinshelwood Model

How to Cite: Kadem, A.J., Lau, X.J., Pung, S.Y., Sreekantan, S., Ramakrishnan, S. (2025). Kinetics Model and Optimization for Photocatalytic Degradation of Methylene Blue over Ag/TiO_2 Catalyst. *Bulletin of Chemical Reaction Engineering & Catalysis*, 20 (3), 517-534. (doi: 10.9767/bcrec.20411)

Permalink/DOI: https://doi.org/10.9767/bcrec.20411

Supporting Information (SI): https://journal.bcrec.id/index.php/bcrec/article/downloadSuppFile/20411/5822

1. Introduction

Wastewater pollution has received significant attention internationally in recent years. Due to the presence of colour in the effluent, waste effluent from industries including dyestuff, textiles, rubber, plastics, leather, cosmetics, and pharmaceuticals might be particularly problematic. The dyestuffs, especially synthetic dyes, have intricate chemical structures and are extremely stable in the presence of oxidising chemicals, heat, and light [1]. Researchers have reported that dyes could put human body health at risk, such as dysfunction of the kidneys, reproductive systems, liver, brain, and central nervous system [1,2]. One method for removing these organic colours from wastewater is the

* Corresponding Author.
Email: srsivakumar@usm.my (S. Ramakrishnan)
§ Both authors contributed equal amount of work.

photocatalytic degradation process by Metal Oxide Semiconductor (MOS) components.

When exposed to enough light, MOS has tremendous potential to produce both oxidising and reducing species. MOS electronic structure is made up of three types of bands, namely a valence band, which is the highest occupied energy band, a conduction band, which is the lowest unoccupied energy band and a band gap, which is a forbidden energy zone. A charge separation event takes place when the incident photons have energy greater than the band gap energy, which results in the creation of a pair of photoexcited electrons and holes. These electron-hole pairs will be contained on the MOS surface after they have formed. They then use the interfacial electron transfer (IFET) mechanism to reduce or oxidise the substrates at an appropriate redox potential [3]. Reaction between the photoexcited electrons and holes with oxygen, water, and hydroxyl groups will produce reactive oxygen species (ROS) namely hydroxyl radicals ($\cdot OH$) and superoxide radical anions ($\cdot O_2^-$) with powerful oxidation capabilities. These ROS play an important role in the degradation of organic contaminants in wastewater [4].

Two important mechanisms are involved in reducing the amount of pollutants in water, which are adsorption and photocatalysis. Mass transfer effects are unavoidable in those situations. Generally, the seven steps for adsorption are as follows: (1) Transportation of the reactants from the bulk phase (boundary layer) to the external surface of the catalyst pellet. It is usually called as film diffusion; (2) Transportation of the reactant from the pore mouth through the catalyst pores to the instant vicinity of the internal catalytic surface. This is the point where the chemical reaction happens. It is usually called as pore diffusion; (3) Adsorption of reactants on the inner catalytic surface; (4) Reaction happens at particular active sites on the catalyst surface; (5) Desorption of the products from the interior surface; (6) Transportation of the products from the internal of the pellet surface to the pore mouth at the external surface; (7) Transportation of the products from the external pellet surface to the bulk fluid. It is usually called as interphase diffusion [5].

Photocatalysis is an advanced oxidation process that relies on the generation of reactive hydroxyl radicals to oxidise the organic matter in water non-selectively at a fast rate [6]. "Catalysis driven acceleration of a light-induced reaction" is the definition of photocatalysis. Before degradation is able to begin, organic contaminants are diffused and absorbed on the photocatalyst's outside surface. Since photocatalytic degradation cannot occur without absorption, the choice and modifications of the absorbent are crucial in this situation.

Among the metal oxide semiconductors, TiO_2 particles are commonly used as photocatalysts for the photocatalysis degradation process. TiO_2 particles have high reactivity under the photon energy of 300 nm < λ < 390 nm and remain stable after repeated catalytic cycles [7]. The chemical and thermal durability of TiO_2 particles also makes them an ideal catalyst with a broad range of applications in photocatalytic water treatment. Additionally, TiO_2 particles are less hazardous and have lower production costs [8,9].

Although TiO_2 has been widely studied as a photocatalyst [10,11], its practical application is limited by several drawbacks. These include its low ability to absorb visible light and the fast recombination of photo-generated electron-hole pairs, which reduces photocatalytic efficiency [12]. Furthermore, high band gap energy resulted in more energy required to be absorbed for the separation of charge carriers [13]. Its wide band gap (roughly 3.2 eV for anatase) requires ultraviolet irradiation for photocatalytic activation, causing very low energy efficiency in utilising solar light [14]. TiO_2 also has limited affinity for certain organic dyes, such as hydrophobic compounds like methylene blue, which further slows down the degradation rate [15]. Modifying TiO_2 with silver (Ag) has shown promise in addressing these limitations [16]. Ag can improve visible-light response by narrowing the effective band gap through plasmonic effects [17], and it helps to reduce electron-hole recombination by forming Schottky barriers at the metal, semiconductor interface [18]. Despite these advances, few studies have systematically investigated how Ag loading, pH, and light source affect photocatalytic activity. Furthermore, kinetic modelling studies, particularly those based on the Langmuir-Hinshelwood (LH) approach, remain limited. For example, Jarandehei et al. focused only on the effect of charge trapping without considering multiple interacting variables [19].

This study aims to fill these gaps by investigating the photocatalytic performance of Ag/TiO_2 under various experimental conditions and by developing a kinetic model using both analytical and numerical methods based on the Langmuir-Hinshelwood framework. A model needs to be generated to understand the kinetics of the photocatalytic degradation. The kinetic model is a simulation and prediction of the behaviour of the photocatalytic degradation system. It can quantitatively describe all the experimental data and simulate its kinetic at different conditions based on the reaction constant. The heterogeneous photocatalytic degradation process generally involved complicated reaction mechanisms with the reactant and the organic solutes adsorbed on the photocatalyst surface. As a basic kinetic equation,

Langmuir–Hinshelwood (LH) kinetics is the most commonly used kinetic expression to explain the kinetics of the heterogeneous catalytic processes [20]. Therefore, this research is an attempt to investigate the kinetic reaction between the dye and the photocatalyst under multiple variables.

This paper involved the synthesis of Ag metal impregnated on TiO_2 as a catalyst for photocatalysis degradation of Methylene Blue (MB), kinetic study and optimisation of operating conditions. The optimization of the photocatalytic degradation of methylene blue (MB) by Ag/TiO_2 catalyst was examined based on three factors, including the concentration of Ag metal impregnated on TiO_2 catalyst and pH value under UV and visible light irradiation. Also, MATLAB was used to create kinetic models that clarified the degradation of MB.

2. Materials and Method

2.1 Materials and Apparatus

Raw materials that were used in this experiment were TiO_2 particles (Merck 100807), $AgNO_3$ particles (Merck 101512), methylene blue (Merck 159270), deionized water, nitric acid (HNO_3) and sodium hydroxide (NaOH). Equipment used in this experiment was UV-Visible Spectrophotometer (Varian Cary 50), FESEM (Zeiss Supra 35VP model), Advanced X-ray Solution D8 Diffractometer (Brucker), Zeta Sizer Nano Series (Malvern) and FT-IR Spectrometer (Perkin Elmer Spectrum One).

2.2 Procedures

To prepare 50 ppm of metal solution, 0.078 g of $AgNO_3$ was mixed with 1000 mL of deionised water and stirred for 2 h. After that, 0.5 g of TiO_2 particles was added into the 500 mL of metal solution and stirred in dark conditions for 30 mins. Then, the mixed solution was stirred under UV light for 1 h. Next, the particles were collected. This was done by centrifuged and dried in oven at 90 ºC for 24 h. After drying, the particles were annealed in a tube furnace to undergo a reduction of metal oxide, producing Ag coupled TiO_2 particles. The particles were heated up at a rate of 10 ºC/min until 500 ºC in an inert atmosphere surrounded by nitrogen gas. The gas flow rate was set as 10 standard cubic feet per hr (SCFH). Next, the particles were soaked at 500 ºC for 2 h using the forming gas which consisted of 5% hydrogen and 95% nitrogen. After soaking for 2 h, the Ag coupled TiO_2 particles were cooled down to room temperature in an inert atmosphere filled with nitrogen gas. The annealing profile was referred to work by a researcher [21]. All the steps were repeated by varying the concentration of $AgNO_3$ solution.

2.3 Photocatalytic Study

5 ppm of MB was prepared by mixing and stirring 0.005 g of MB powder in 1000 mL of distilled water. Next, 0.1 g/L of Ag/TiO_2 catalyst was prepared by dispersing 0.025 g of Ag/TiO_2 catalyst into 250 mL of MB solution. The mixture was magnetically stirred in dark conditions for 30 mins and in light conditions (either UV or visible light) for 1 h. The stirring action in dark conditions was aimed to ensure the absorption-desorption equilibrium state of MB on the surface of Ag/TiO_2 catalyst was reached before illumination of light. The solution was sampled at every 15 mins intervals into cuvette for UV-Vis spectroscopy measurement. The variables that were studied in this work were concentration of $AgNO_3$ solution, pH of the solution and light. Concentration of $AgNO_3$ were 20 ppm, 50 ppm and 80 ppm. The pH of solutions were adjusted to 5 (acidic), 7 (neutral) and 9 (alkaline). The optical excitation light sources were visible light and UV light. The sequence of the experiment was generated by Minitab 18 (statistical software) based on Design of Experiment (DOE) to ensure the randomness of the experiment and avoid any biasness. Table 1 shows the sequence of the experiment collected according to DOE generated by Minitab.

2.4 Characterizations

The synthesized metal oxide coupled TiO_2 particles were subjected to several characterization techniques to obtain various

Table 1. Experimental sequence of photocatalytic study of Ag/TiO_2 catalyst.

$AgNO_3$ concentration (ppm)	pH	Light
50	5	Visible light
20	5	UV light
20	9	UV light
80	7	Visible light
80	5	UV light
80	7	UV light
20	5	Visible light
50	9	UV light
20	7	Visible light
20	9	Visible light
50	7	Visible light
50	9	Visible light
80	5	Visible light
80	9	UV light
50	7	UV light
50	5	UV light
20	7	UV light
80	9	Visible light

information about the particles. The particles were examined by field emission scanning electron microscopy (FESEM FEI Quanta 650 FEG SEM), energy dispersive x-ray spectrophotometer (EDX) that couples with FESEM to analyze the sample's elemental composition, and X-Ray Diffraction (XRD Bruker D8 diffractometer).

FTIR was conducted to determine the functional groups for the sample. Firstly, the particles were grinded together with Potassium bromide. Potassium bromide was chosen because of its transparency in the infra-red region. After grinding, the sample was made into a transparent pellet by hydraulic press at 2000 psi for 2 mins. Lastly, the samples were measured using FTIR with wavelength start from 4000 to 400 cm^{-1} and resolution of 4 cm^{-1}.

Zeta potential of the particles is also determined. First, 0.002 g of Ag/TiO_2 catalyst were added to 20 mL of deionized water. Next, the mixture was sonicated for 20 mins to ensure the particles were well dispersed in the deionized water. After that, the mixed particles were put inside the Malvern Zeta Sizer Nano series to determine its zeta potential.

2.5 Photocatalytic Properties

UV–Vis spectroscopy measurements were performed by using Perkin Elmer Lambda 35 UV Spectrophotometer to measure the absorption characteristics of the MB solution degraded by TiO_2 and Ag/TiO_2 catalyst in the range of 200 nm to 800 nm wavelength at fast scan rate. Before cuvette was put inside the spectrophotometer, the cuvette must be wipe with tissue paper to ensure the surface of cuvette was clean from any dust or fingerprint. A fingerprinted cuvette would cause a higher absorbance measurement, and the recorded concentration would be much greater than the real concentration.

2.6 Kinetic Modelling using Power Law Model Based on the Langmuir-Hinshelwood Framework

In this work, kinetic modelling was generated based on Langmuir-Hinshelwood equations by using MATLAB to emulate the reaction of the photocatalytic degradation of MB by Ag/TiO_2 catalyst. MATLAB is a programming tool that enables the incorporation of numerical computation, symbolic computation, graphics, and programming. This programming tool has been employed to derive the Langmuir-Hinshelwood algorithms and to compute mathematical computations.

3. Result and Discussion

3.1 Structural and Morphological Analyses

Figure 1 illustrates XRD patterns of TiO_2 particles and Ag/TiO_2 catalyst before and after annealing process at 500 °C, whereas Figure 2 shows the XRD patterns for the various concentration of Ag metal coupled on TiO_2 catalyst. The diffraction pattern matched well with anatase TiO_2 particles (ISCD 98-007-6028). The diffraction angle and miller indexes of the anatase TiO_2 particles were labelled in Table 2.

No diffraction peak was found from brookite or rutile phase of TiO_2 particles. All Ag/TiO_2 catalyst produced using different concentrations

Table 2. Diffraction angle and miller indices of the anatase TiO_2 particles.

Diffraction angle, 2θ	*h*	*k*	*l*
25.34°	0	1	1
36.99°	0	1	3
37.83°	0	0	4
38.60°	1	1	2
48.07°	0	2	0
53.93°	0	1	5
55.10°	1	2	1

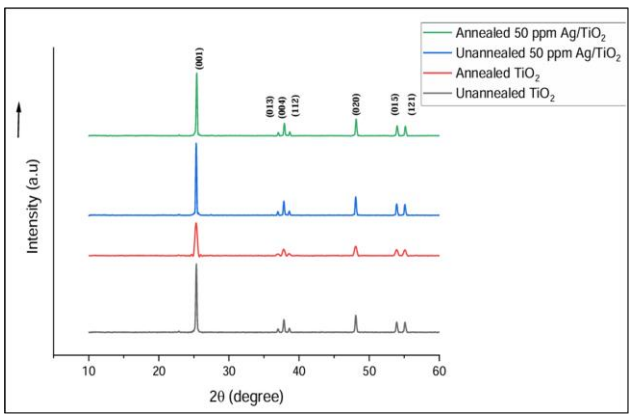

Figure 1. XRD patterns for TiO_2 particles and Ag/TiO_2 catalyst before and after annealing at 500 °C.

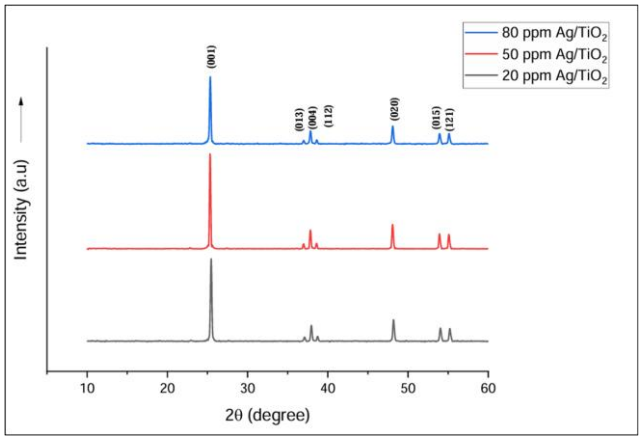

Figure 2. XRD patterns of Ag/TiO_2 catalyst prepared using various concentrations of $AgNO_3$ solution.

of Ag metal, solutions such as 20, 50 and 80 ppm, show similar XRD patterns. Peak intensity for annealed TiO_2 particles at 25.340 was lower compared with unannealed TiO_2 particles. This might be due to the presence of lattice defect, such as micro strain, which causes the peak broadening and lowers the peak.

Deposition of Ag metal using the impregnation method could produce AgO on the surface of TiO_2 particles. Thus, the Ag/TiO_2 catalyst were annealed at 500 ^{0}C in reductive atmosphere using forming gas (95% N_2 and 5% H_2) in order to reduce AgO (if there was any) to Ag. However, it is also a concern that TiO_2 particles would have the possibility to be reduced to Ti during annealing. Since the XRD pattern of annealed TiO_2 particles did not find any diffraction peaks related to Ti, it can be concluded that annealing of Ag/TiO_2 catalyst at 500 ^{0}C for 2 h did not reduce TiO_2 particles to Ti. No Ag diffraction peak was observed in Figure 1 and Figure 2, regardless of the concentration of $AgNO_3$ used in the impregnation process. The presence of Ag on the surface of TiO_2 particles might be below the detection limit of XRD. Although the Ag/TiO_2 catalyst showed similar XRD patterns, all samples were composed of the anatase phase. This is a favorable characteristic for wastewater treatment applications, as anatase is well known for its excellent photocatalytic properties. Unlike rutile, which has a direct bandgap, anatase has an indirect bandgap structure. This indirect bandgap leads to longer lifetimes of electron-hole pairs (e^-/h^+), which reduces their recombination and improves photocatalytic efficiency [22].

Figure 3 shows the morphology of TiO_2 particles before annealing while Figure 4 shows the morphology of TiO_2 particles after annealing at 500 ^{0}C for 2 h of soaking time in ambient. There is no much difference between the morphology of TiO_2 particles before and after annealing based on the SEM images. In addition, by comparing the FESEM images between TiO_2 particles and Ag/TiO_2 catalyst (Figure 5 to Figure 8), the coupling of Ag did not affect the spherical shape of TiO_2 particles.

As shown in Figure 9, the average particle size of TiO_2 particles remains unchanged after annealing. The same situation is applied to annealing of Ag/TiO_2 catalyst. Nevertheless, it is

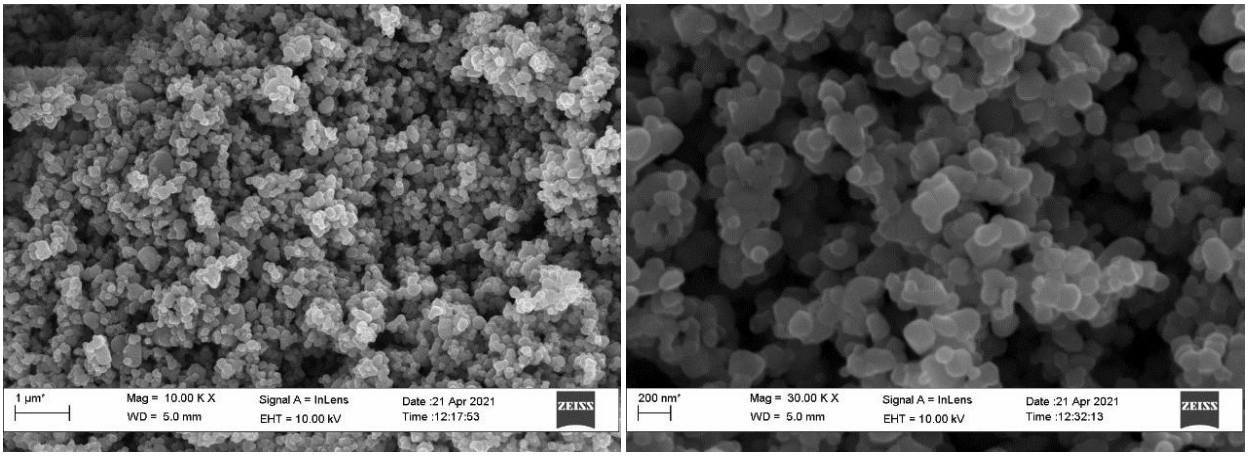

Figure 3. SEM images of unannealed TiO_2 particles at magnification of (a) 10 kX and (b) 30 kX.

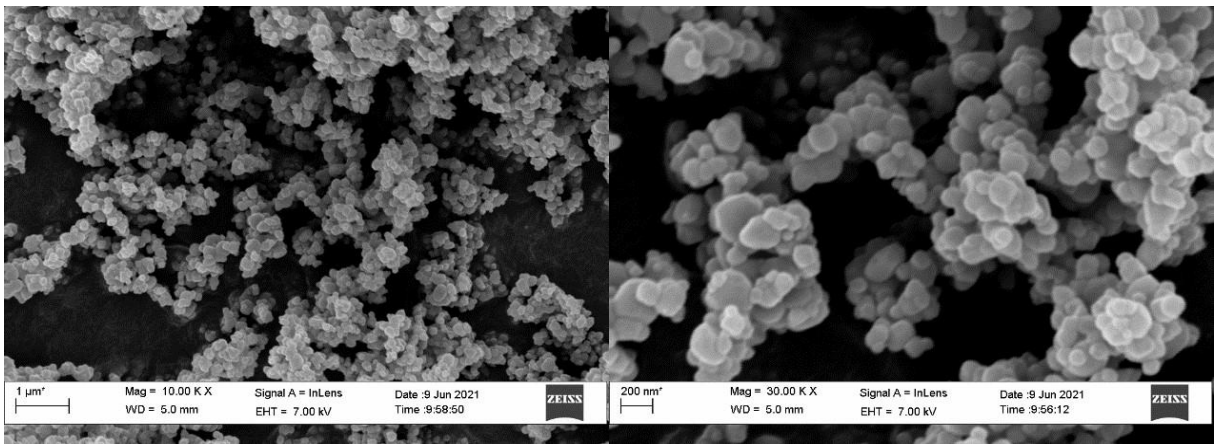

Figure 4. SEM images of annealed TiO_2 particles at 500 ^{0}C for 2 h of soaking time at magnification of (a) 10 kX and (b) 30 kX.

noted that there was a slight decrease of TiO_2 particles size after deposition of Ag. For instance, the average particle size decreased from 184.02 nm to 174.56 nm when the concentration of $AgNO_3$ solution increased from 20 ppm to 80 ppm. There may be a slight distortion of the crystal lattice that results in a decline in the crystal growth as the concentration of Ag metal increases, as demonstrated by Komaraiah and his coworkers in their study [23]. A slight decrease in particle size with increasing Ag concentration suggests that potential surface modification could improve

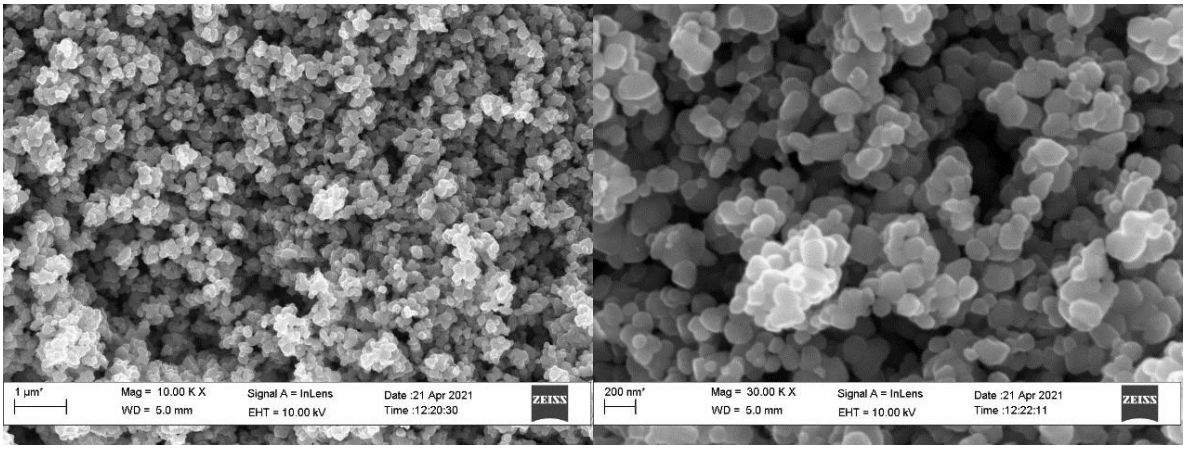

Figure 5. SEM images of annealed 20 ppm Ag metal coupled on TiO_2 particles at 500 ^oC for 2 h of soaking time at magnification of (a) 10 kX and (b) 30 kX.

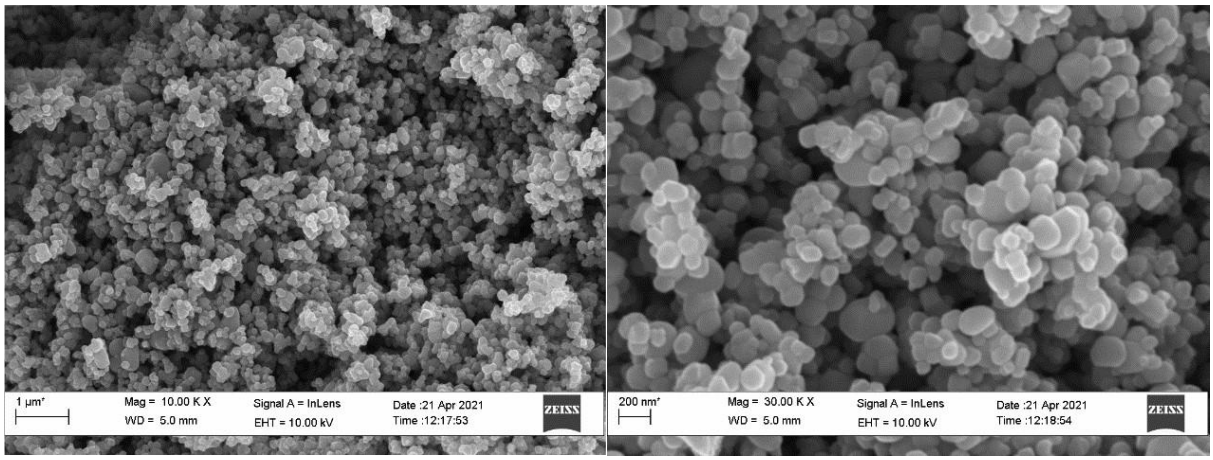

Figure 6. SEM images of unannealed 50 ppm Ag metal coupled on TiO_2 particles at magnification of (a) 10 kX and (b) 30 kX.

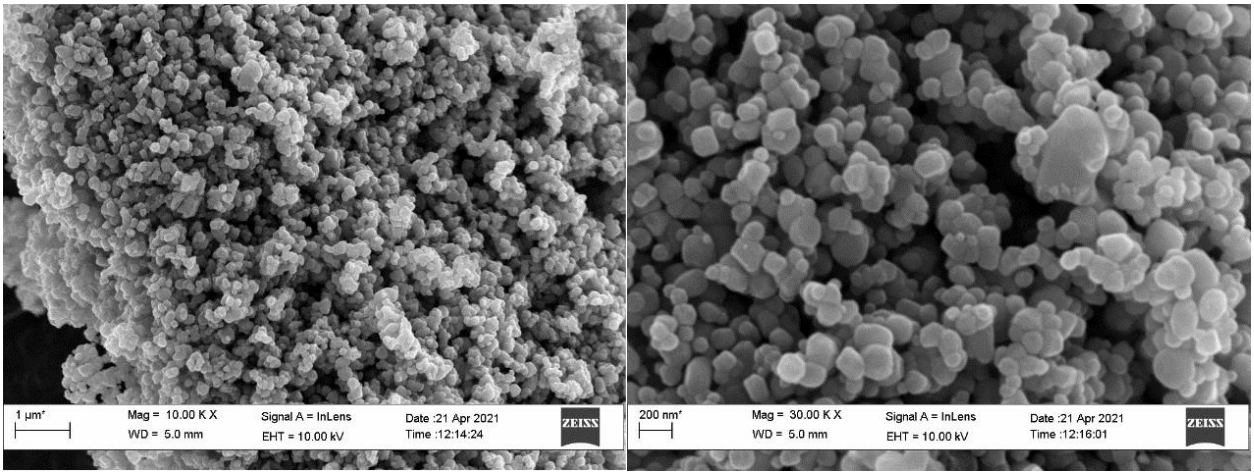

Figure 7. SEM images of annealed 50 ppm Ag metal coupled on TiO_2 particles at 500 ^oC for 2 h of soaking time at magnification of (a) 10 kX and (b) 30 kX.

photocatalytic performance. This is because smaller particle sizes increase the specific surface area, providing more active sites for light absorption and redox reactions, thereby enhancing photocatalytic efficiency [24].

Two sample t-tests are conducted to determine if there is any difference in means of particles size for unannealed TiO_2 particles and annealed TiO_2 particles. The p-value is bigger than 0.05, the significant level, as shown in Figure S1 (Supporting Information). Therefore, it can be concluded that there is no statistical difference between the size of unannealed TiO_2 particles and annealed TiO_2 particles. The annealing process did not change the size of TiO_2 particles significantly.

Figure 10 (a) shows the EDX analysis of annealed TiO_2 particles. The atomic percent of Ti and O are 37.11 % and 62.89 %, respectively. The result shows that the annealed TiO_2 particles were lack of oxygen. No Ag and other impurities were detected on the annealed TiO_2 particles, suggesting that the annealing process did not introduce contamination on the TiO_2 particles. Figure 10 (b) shows the Ag atomic percent of Ag/TiO_2 catalyst prepared using different concentrations of $AgNO_3$ solution. The amount of Ag detected from the samples increased with increasing concentration of $AgNO_3$ solution. It is recorded the highest atomic percent of Ag 1.89 % when the particles were prepared using 80 ppm of $AgNO_3$ solution.

Fourier transform infra-red (FTIR) spectral analysis of the annealed TiO_2 particles and Ag/TiO_2 catalyst was performed using KBr pellets in a spectrometer within the 400-4000 cm^{-1}

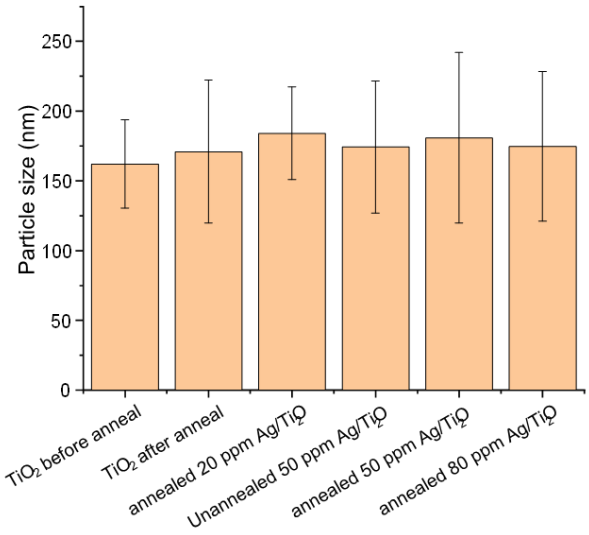

Figure 9. Average particle size of TiO_2 particles and Ag/TiO_2 catalyst.

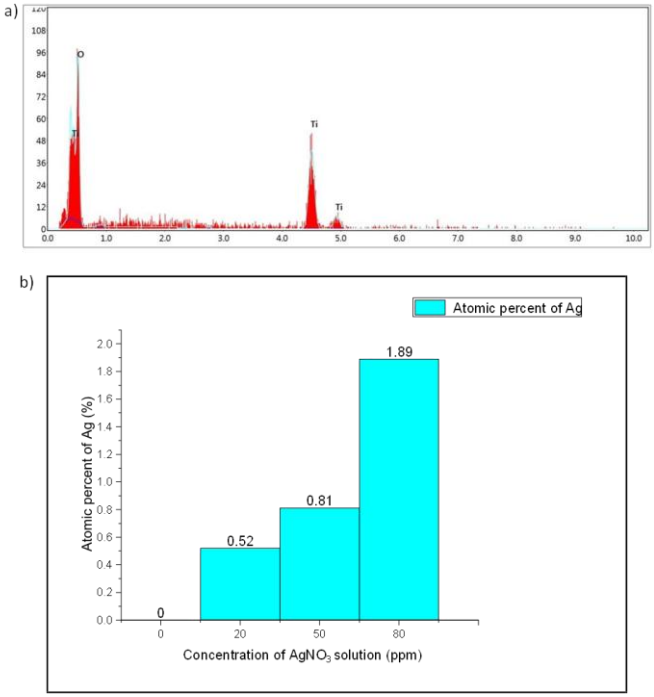

Figure 10. (a) EDX analysis of annealed TiO_2 particles and (b) atomic percent of Ag as a function of concentration of $AgNO_3$ solution.

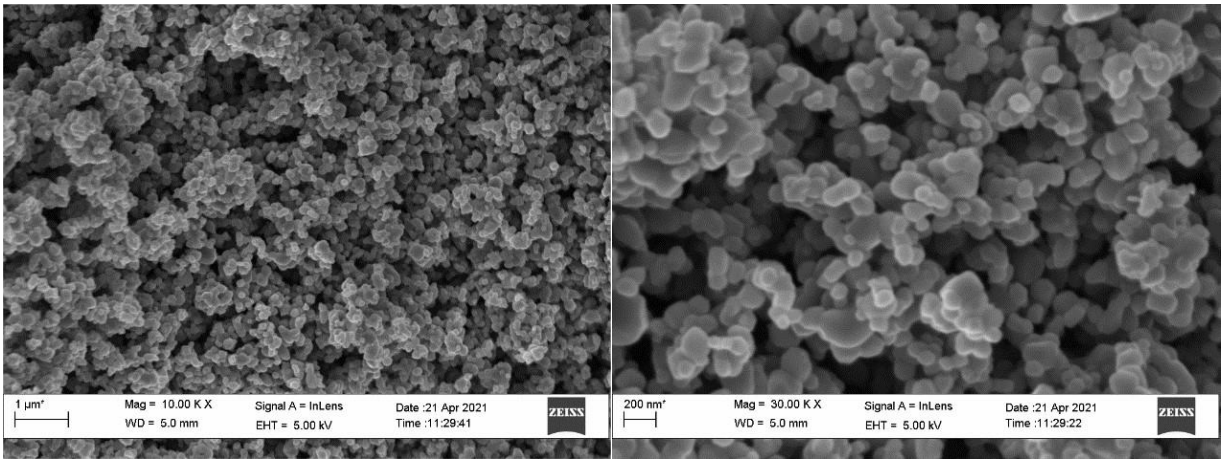

Figure 8. SEM images of annealed 80 ppm Ag metal coupled on TiO_2 particles at 500 ^{0}C for 2 h of soaking time at magnification of (a) 10 kX and (b) 30 kX.

wavenumber range. The FTIR spectra was shown in Figure 11. The strong absorption peak around 400-500 cm^{-1} represents to the characteristic vibrations of Ti-O-Ti lattice and bending mode of vibrations [25]. The peak at 700 and 800 cm^{-1} were attributed to the stretching vibrations of Ti-O bonds in the TiO_2 particles lattice [25]. In addition, there is also a peak around 1600-1700 cm^{-1}, showing the bending vibrations of the O-H bending. The bending was responsible for the absorption of hydroxyl ions on the surface of catalyst [26]. As highlighted in Figure 11 (b), there is a shift of 52 cm^{-1} on the TiO_2 particles lattice vibration. This could be the effect of Ag coupling on the TiO_2 particles, forming bonding of Ag/TiO_2 catalyst. Importantly, the presence of O-H bending vibrations around 1600-1700 cm^{-1} indicates surface hydroxyl groups. These hydroxyl groups play a pivotal role in photocatalysis: they act as active sites for trapping photogenerated holes and generating hydroxyl radicals (•OH), which are potent oxidizing agents in the degradation of organic pollutants [27].

The observed 52 cm^{-1} shift in the Ti-O-Ti lattice vibration upon Ag loading suggests an interaction between Ag and the TiO_2 lattice. This interaction implies successful doping or surface modification, which alters the local electronic environment of TiO_2. Such modifications can enhance charge separation efficiency by acting as electron sinks, thereby reducing electron-hole recombination. Zeta Potential is a measure of the electrostatic interactions between particles and can be used to predict dispersion stability. The magnitude of the zeta potential gave an indication of the potential stability of the TiO_2 particles photocatalyst in water. In an aqueous system, the particles are considered as stable when their zeta potential is more positive than +30 mV or more negative than -30 mV. The zeta potentials of all samples are presented in Figure 12. All the zeta potentials are within the ± 30 mV range and therefore they are considered unstable. This can be proven through the FESEM images in Figures 3 to 8, which shows agglomeration of the particles. All of the TiO_2 particles and Ag/TiO_2 catalysts show a negative magnitude of zeta potential, which suggests that they were negatively charged. Therefore, they were suitable to degrade MB as it is a cationic dye. The negative surface charge facilitates electrostatic attraction between the catalyst surface and the positively charged MB molecules, enhancing the adsorption of the dye onto the catalyst surface. This increased adsorption improves the availability of MB molecules at the active sites of the photocatalyst, thereby promoting more efficient photodegradation under light irradiation [28].

3.2 Photocatalytic Performances of TiO_2 Particles and Ag/TiO_2 Catalyst

3.2.1 Photocatalytic properties of TiO_2 particles

The photocatalytic activity of TiO_2 particles was measured as a control in this research. Figure 13 (a) and (b) show the absorption spectra of 5 ppm MB with the presence of unannealed and annealed TiO_2 particles under UV light, respectively. It is observed that the maximum

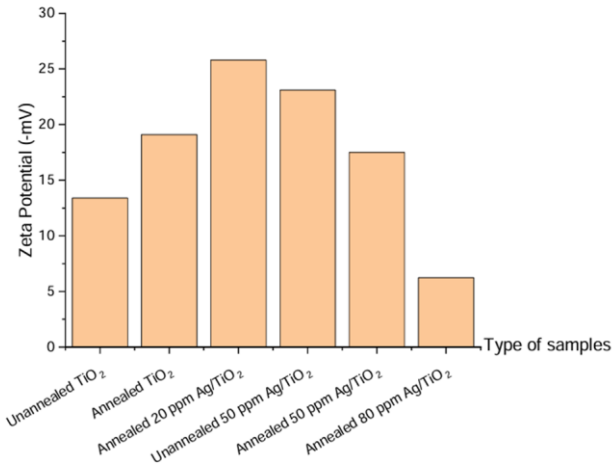

Figure 12. Zeta potential of TiO_2 particles and Ag/TiO_2 catalyst.

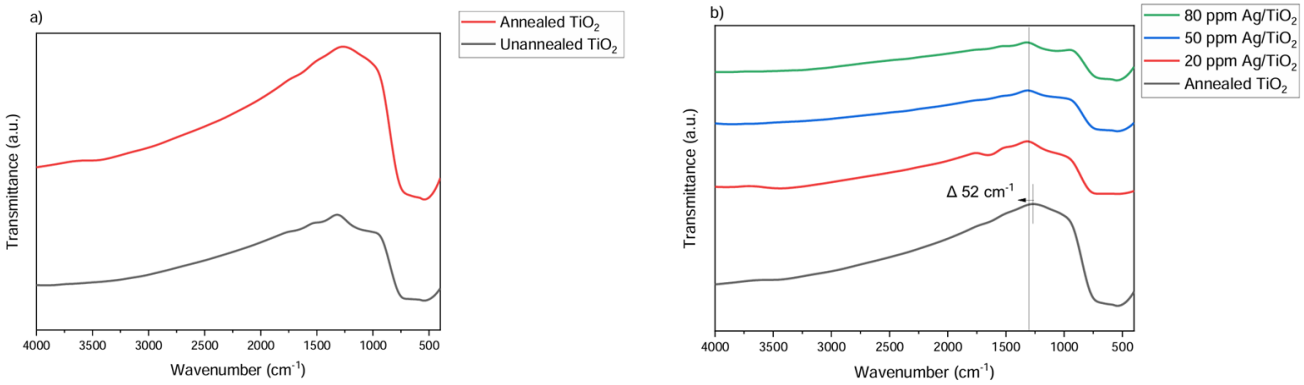

Figure 11. FTIR spectra of: (a) unannealed and annealed TiO_2 particles; (b) various concentration of Ag metal coupled on TiO_2 particles.

absorbance peak, i.e. 663 nm, decreases gradually as duration of UV light irradiation increases. Figure 13 (c) shows the photodegradation efficiency (PE) of TiO_2 particles under UV light. It degraded to 82.62% and 81.71% of MB after 60 mins under UV light irradiation for unannealed and annealed TiO_2 particles, respectively.

Figure 13 (d) shows the plot of ln (*Ao*) vs *t*. The linear fitting of the plot indicates that the photodegradation of MB by unannealed TiO_2 particles under UV light followed 1st order kinetics. The rate constants, which could be determined from the slope of the plot, are 0.03064 min^{-1} and 0.02929 min^{-1}, respectively. The results suggest that annealing at 500 °C did not affect the photocatalytic performances of TiO_2 particles significantly.

3.2.2 Photocatalytic performances of Ag/TiO_2 catalyst under UV light

Figure 14 shows the photodegradation efficiencies of Ag/TiO_2 catalyst with different concentrations under UV light. In 20 ppm of Ag metal solution concentration, the photodegradation efficiency (PE) decreases from 83.30% to 69.37% with increasing pH value. While in 50 ppm and 80 ppm, at higher pH value the PE are almost the same. However, both 50 ppm and 80 ppm share the similarity that in pH of 5, the PE is the highest which accounts for 83.82% and 82.12% respectively. Generally, the Ag/TiO_2 catalyst prepared using 50 ppm of $AgNO_3$ solution, under pH of 5 has the best photocatalytic performance. The Ag/TiO_2 catalyst recorded of 83.82% PE, which is higher than that achieved by the TiO_2 particles (82.62%).

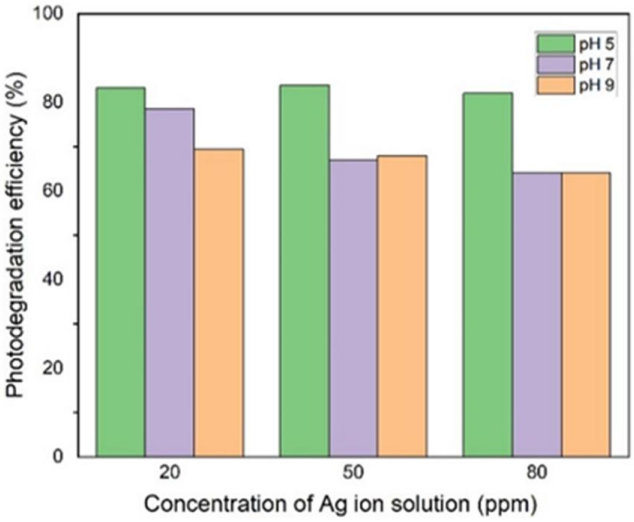

Figure 14. Photodegradation efficiencies of Ag/TiO_2 catalyst under exposure of UV light with different Ag concentrations and different pH solutions.

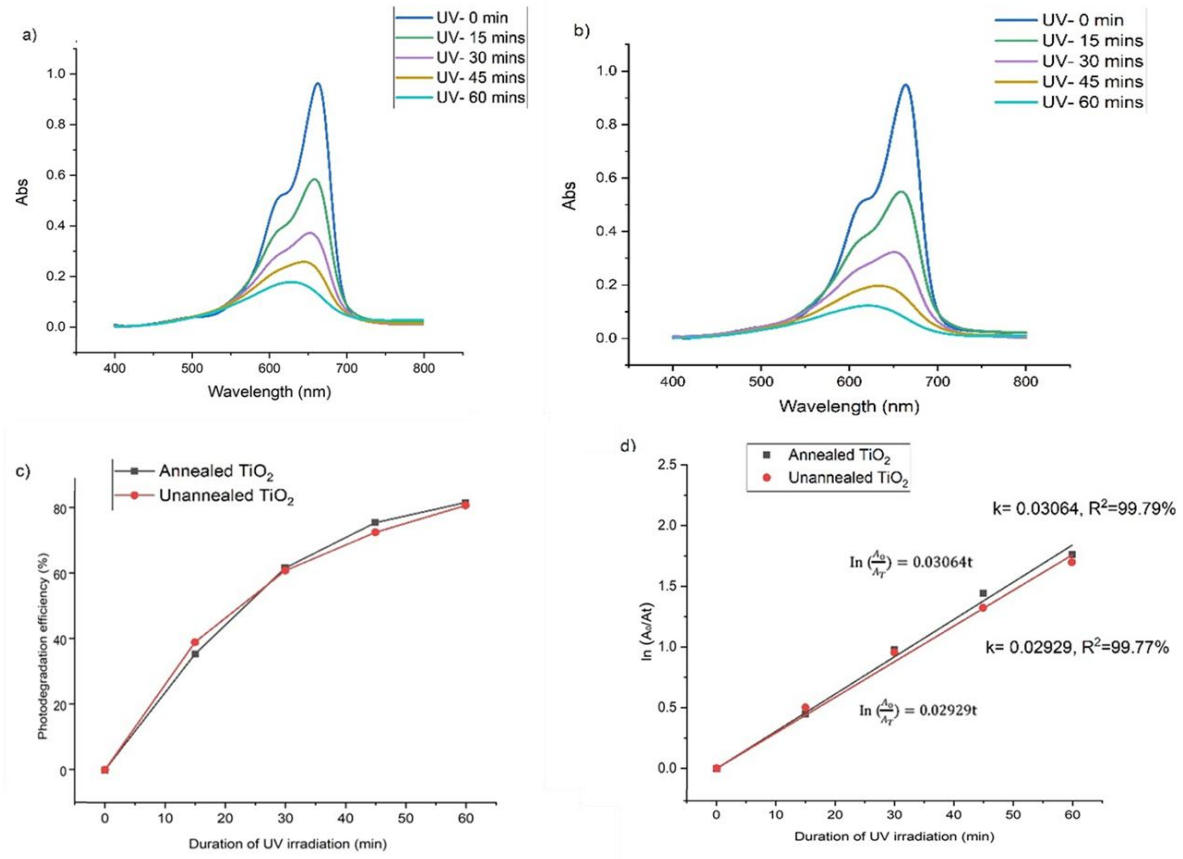

Figure 13. UV-Vis spectra for methylene blue photodegraded by (a) unannealed TiO_2 particles and (b) annealed TiO_2 particles under UV light; (c) photodegradation efficiencies and (d) kinetic plot.

Figure 15 shows the rate constant of Ag/TiO_2 catalyst synthesized using different Ag metal concentration under UV light. The rate constant is an indication of how fast the MB was degraded by the photocatalysts. The highest rate constant obtained is 0.03298 min^{-1} for Ag/TiO_2 catalyst synthesized using 50 ppm Ag metal in pH of solution and is 1.84 times better than the lowest rate constant. The smallest rate constant (0.01792 min^{-1}) was recorded by Ag/TiO_2 catalyst synthesized using 80 ppm Ag metal solution and tested in pH of 7 solution.

It is worth noting that EDX analysis confirmed the successful loading of silver onto the surface of TiO_2. The enhanced photocatalytic performance observed at the optimum Ag concentration (50 ppm) is attributed to the presence of silver, with EDX showing an atomic percent of 0.81% in this sample. At this level, silver acts as an electron trap, reducing charge recombination, thereby improving photocatalytic efficiency. However, when the silver content was increased to 80 ppm, EDX showed a higher Ag atomic percent of 1.89%, but the photocatalytic efficiency slightly declined. This decline in efficiency may result from increased light scattering and agglomeration of particles [25]. It is therefore suggested that the effect of pH and concentration of Ag metal on the photocatalytic performances of Ag/TiO_2 catalyst was due to the same mechanism as explained below:

(a) Effect of concentration of Ag metal:

There are a few possible explanations if coupling of Ag on TiO_2 particles. Coupling of Ag on TiO_2 particles could change the active sites available and the number of absorbed photons. In addition, Ag deposited on the surface of TiO_2 particles could act as electron traps, facilitating electron hole pair separation due to formation of a Schottky barrier at the metal-semiconductor contact region [29]. As a result, the charge carrier recombination is suppressed, which in turn generates more powerful oxidizing free radicals. It then leads to superior photocatalytic performances of Ag/TiO_2 catalyst.

In contrast, coupling of Ag on the surface of TiO_2 particles could result in light scattering and aggregation of the catalyst particles [25]. Excessive coverage of TiO_2 particles with Ag particles might limit the amount of light reaching to the surface of TiO_2 particles thus reducing the number of photogenerated electron-hole pairs. Also, the number of active sites decreased due to the agglomeration of TiO_2 particles [25,30,31].

(b) Effect of pH of solution:

In this research, the photocatalytic degradation of MB was more effective in acidic solution (pH = 5). This behaviour may be described on the basis that it was due to the increased availability of OH^- ions at low pH values. By interacting with holes, the OH^- ions created additional hydroxyl radicals, which were thought to be responsible for photocatalytic degradation. The adsorption on Ag/TiO_2 catalyst is predominantly determined by its surface properties, and surface reactivity is substantially determined by surface hydroxyl groups. The result is in line with the work done by Kulkarni and his co-workers [32].

However, the finding is also in contrast with studies conducted by other researchers. They deduced that photodegradation rate of MB increases as the pH value increases. As MB is cationic dye, therefore, the alkaline condition favours the adsorption of MB on Ag/TiO_2 catalyst surface. The Ag/TiO_2 catalyst has zero-point charge at pH of 6, as suggested by Lantos and his co-workers [33]. Therefore, at acidic condition, particle surface is positively charged, whereas at basic condition it is negatively charged. Therefore, in alkaline conditions, negative charges increase on the surface area of the photocatalyst, which enhances the MB adsorption. The acidic solution, on the contrary, will prevent adsorption. In addition, the $OH\cdot$ free radicals can form alkaline solution more easily because of the oxidation of OH ions. Therefore, the degradation efficiency increased with increasing pH [25,34,35].

3.2.3 Photocatalytic performances of Ag/TiO_2 catalyst under visible light

Figure 16 shows the PEs of Ag/TiO_2 catalyst synthesized using different Ag metal concentrations under visible light. It can be shown that under 20 ppm Ag metal solution, the PE decreases from 39.41%, 18.21% then to 7.42% when pH decreases from 5, 7 to 9. However, under 50 ppm Ag metal solution, PE is the highest in

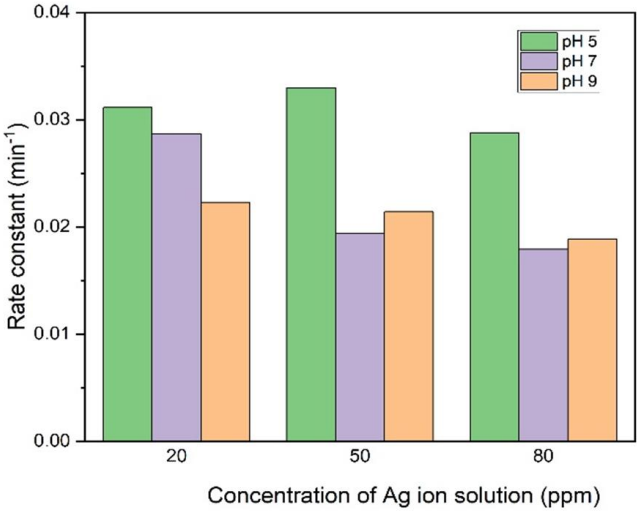

Figure 15. Rate constants of Ag/TiO_2 catalyst under exposure of UV light with different Ag concentrations and different pH solutions.

neutral condition which is 32.15% and acidic conditions show the lowest efficiency (8.74%). Meanwhile, the PE shows an increasing trend in 80 ppm Ag metal solution from 4.48%, 11.83% to 21.29% with increasing pH. It is noticed that in pH of 5 the PE shows extreme behaviour. Under the acidic condition (pH of 5), the PE is overall the highest when concentration is 20 ppm (39.41%) and the overall lowest when concentration is 80 ppm (4.48%). Nevertheless, the PE remains the same which are 21.23% and 21.29% respectively when concentration of Ag metal solution increases from 50 ppm to 80 ppm under alkaline conditions. Figure 17 shows the rate constant of Ag/TiO_2 catalyst under visible light. The rate constant shows the exact trend with the PE as discussed above.

It is noted that the overall photocatalytic performance of Ag/TiO_2 catalyst in visible light irradiation was poorer than in UV light. Under UV light irradiation, the Ag/TiO_2 catalyst received light energy that is greater than its band gap energy. The optically excited electrons were able to reduce the dissolved oxygen in order to produce superoxide radicals. Meanwhile, holes were in charge of the formation of hydroxyl radical. Both superoxide radicals and hydroxyl radicals were strong oxidants which then able to degrade the MB effectively [36]. In contrast, when Ag/TiO_2 catalyst was irradiated under visible light, the degradation profile of MB dyes was then very much dependent only on the electronic transition of organic dyes [37].

The visible light did not have sufficient energy to optically excited Ag/TiO_2 catalyst. It is therefore unable to generate any electron-hole pairs. The results in Figure 16 show that Ag/TiO_2 catalyst is still capable of degrading MB. This may be due to self-sensitization of MB. MB is said to be activated under visible light but not Ag/TiO_2 catalyst. Excited MB molecules then injected electrons into the conduction band of Ag/TiO_2 catalyst. The injected electrons were responsible for the reduction of dissolved oxygen to superoxide and hydroxyl radicals [38]. It is also important to note that while this study focused on the photocatalytic degradation of methylene blue under UV and visible light, we acknowledge that a control experiment conducted under full dark conditions would provide additional insight and should be considered in future studies.

3.3 Local Optimization of Photocatalytic Performance of Ag/TiO_2 Catalyst

Pareto charts of photodegradation efficiency (PE) and rate constant (RC) over the responses were plotted as shown in Figure 18. The Pareto chart was used to differentiate the relative magnitude and the statistical significance of both main and interaction effects. The Pareto chart and ANOVA Tables (S1 and S2, Supporting

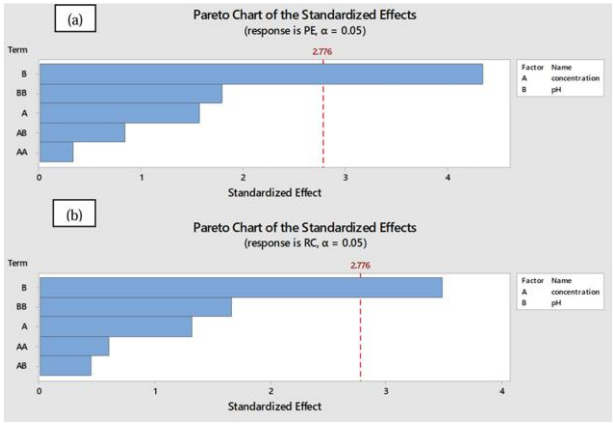

Figure 18. Pareto chart for a) PE and b) RC.

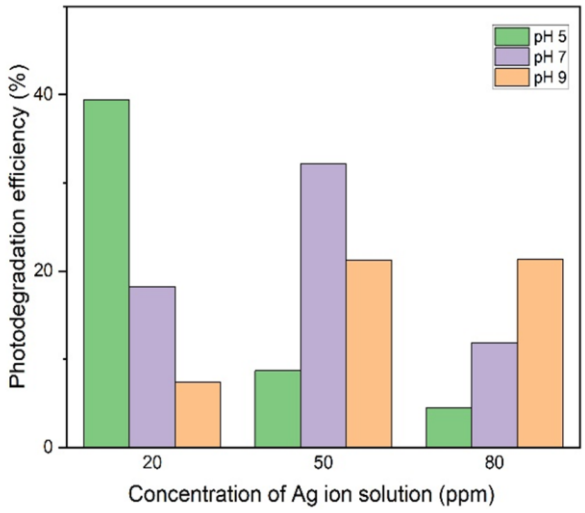

Figure 16. Photodegradation efficiencies of Ag/TiO_2 catalyst under exposure of visible light with different Ag concentrations and different pH solutions.

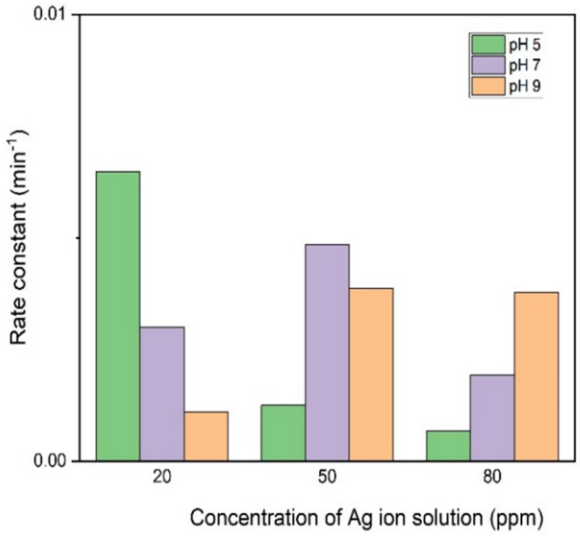

Figure 17. Rate constants of Ag/TiO_2 catalyst under exposure of visible light with different Ag concentrations and different pH solutions.

Information) confirmed that pH was the only factor with a significant effect on RC and PE. Figure 19 shows the contour plots and surface plots for PE and RC. As the green colour goes darker, the higher will be the value for the responses. It shows that low pH region is the best condition for photocatalytic degradation to occur since the PE and RC are higher values at this region. It is also in agreement with the pareto effect chart as mentioned previously that pH plays significant role in degradation of MB. Figure 20 demonstrates the response optimizer generated by Minitab 18. The optimal parameters are determined by maximizing the composite desirability which in this case is 0.9716. Response optimizer gives the optimum parameters for Ag/TiO_2 catalyst to have the highest rate constant and PE, which are in 22.6263 ppm Ag metal solution concentration and pH of 5. It is predicted with such conditions the PE and rate constant can be reached up to 84.0006 % and 0.0321 min^{-1}. All of the responses were given equal weight, and the default value for d = 1 was set to 1.0.

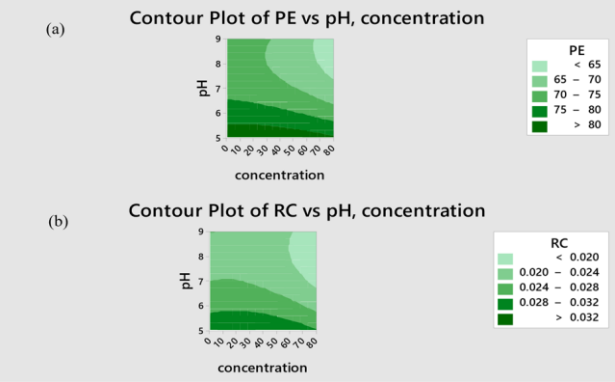

Figure 19. a) Contour plots of PE vs pH and $AgNO_3$ concentration (ppm), b) Contour plots of RC vs pH and $AgNO_3$ concentration (ppm).

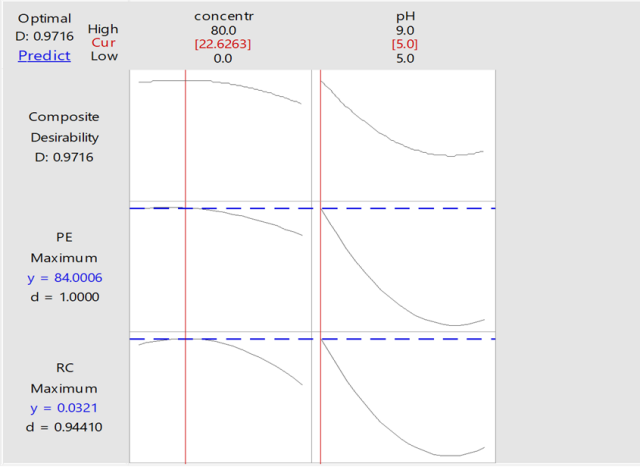

Figure 20. Response optimizer plot for parameters $AgNO_3$ concentration (ppm) and pH influencing the PE and RC.

3.4 Comparison of Predicted Model and Experimental Model

The photocatalytic degradation rate of MB has been modelled successfully by Power Law kinetic models. In order to solve the nonlinear differential equation, which is the LH equation, two methods were implemented which are the numerical and analytical methods. A dynamic model was generated to understand the behaviour of pH and the concentration of Ag metal on photocatalytic activity. The model was simulated and analysed for Ag/TiO_2 catalyst, which acts as a photocatalyst for the LH kinetic framework.

The expression of r as Langmuir-Hinshelwood (LH) kinetic rate law, as stated below in Eq. 1, has been employed to describe the observed photocatalytic degradation rate. In these kinetic models, experimental results of photocatalytic degradation of MB were taken and fitted to Power Law numerical and analytical models. The function *ode45* in MATLAB software has many distinct functions to solve ordinary differential equations numerically (ODEs). The coding in the MATLAB program was listed in Supporting Information. Meanwhile, Perturbation-Iteration Algorithm (PIA) was used to solve the equation analytically by using reaction rate constants k_r, absorption coefficient K and the initial concentration C_o, PIA equation, as shown in Eq. 2, was used:

$$-\frac{dC}{dt} = r = \frac{k_r KC}{1+KC} \quad (1)$$

$$C = C_o e^{-krKt}[(1 + \varepsilon C_o K(1 - e^{-k_r Kt})] \quad (2)$$

These models were used to analyse photocatalytic reactions over different concentration vs time. One advantage of formulating the rate forms from representative assumptions as opposed to empirical observations lies in the ability to predict trends or values for the parameter groups obtained (absorption coefficient (K) and reaction rate constant (k_r)). Importantly reaction rate constant (k_r) is estimated to be a function solely of catalyst characterisation and reaction circumstances, and thus its value should be unaffected by the degraded organic reactant. The kinetic data of the Ag metal in a specific pH under UV irradiation were correlated with the LH Model as shown in Eq. 3:

$$\frac{C}{r} = \frac{1}{k_r K} + \frac{C}{k_r} \quad (3)$$

According to Eq. 3, the rate of reaction can be found by finding tangent line which represents the relationship between the ratio of concentration to the reciprocal rate constant to concentration. It enables the simultaneous

determination of the absorption coefficient (K) and reaction rate constant (k_r) from the slope and intercept of the plot $\frac{C}{k_r}$ and $\frac{C}{r}$. For example, using Eq. 3, a linear fitting of the ratio of concentration to rate against concentration line graph for 20 ppm Ag metal solution at pH of 5 under UV irradiation can be plotted as shown in Figure 21. Based on this linear fitting line, the gradient was found to be 1.275. Using Eq. 3, the k_r can be derived as 0.784, as the inverse gradient of 1.275 in Figure 21. Subsequently, the K value can be determined, which is 0.053 in this case.

The rate of photodegradation of MB is shown to follow the first-order reaction kinetics (Figures S2 to S7, Supporting Information). For a pseudo-first-order reaction, KC is very small compared to 1. Therefore, Eq. 1 reduces to:

$$\frac{dC}{dt} = -k_r\, KC \tag{4}$$

$$\frac{dC}{dt} = -k_1 C \tag{5}$$

$$C(t) = C_o e^{-k_1 t} \tag{6}$$

where $k_1 = k_r K$ is the apparent first-order reaction rate constant.

Figures 22 to 24 show the degradation of MB by Ag/TiO_2 under various concentrations and pH. The lines represent models while the dots represent the experimental data. It is evident that both the analytical and numerical models provide a reasonable fit to the experimental results. However, the numerical method demonstrates better agreement with the experimental data compared to the analytical method. Overall, the results indicate that the concentration of MB follows a first-order exponential decay, showing a decreasing trend from its initial concentration. Furthermore, the experimental data can generally be described well by the Langmuir adsorption isotherm model.

The experimental degradation efficiency of Ag/TiO_2 catalyst was also compared with the predicted modelling degradation efficiency. The photodegradation efficiency (PE%) was calculated as below:

$$PE = \frac{C_o - C_t}{C_o}\, x\, 100\% \tag{7}$$

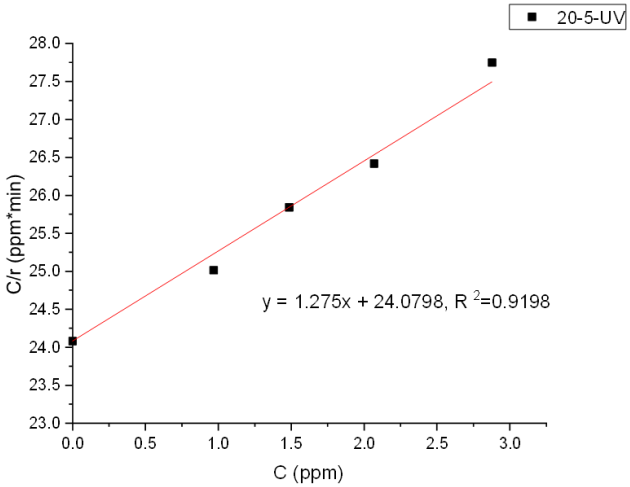

Figure 21. Experimental plot of ratio of MB concentration (mg/L) to reciprocal rate against concentration at 20 ppm Ag metal solution in pH of 5 under UV irradiation.

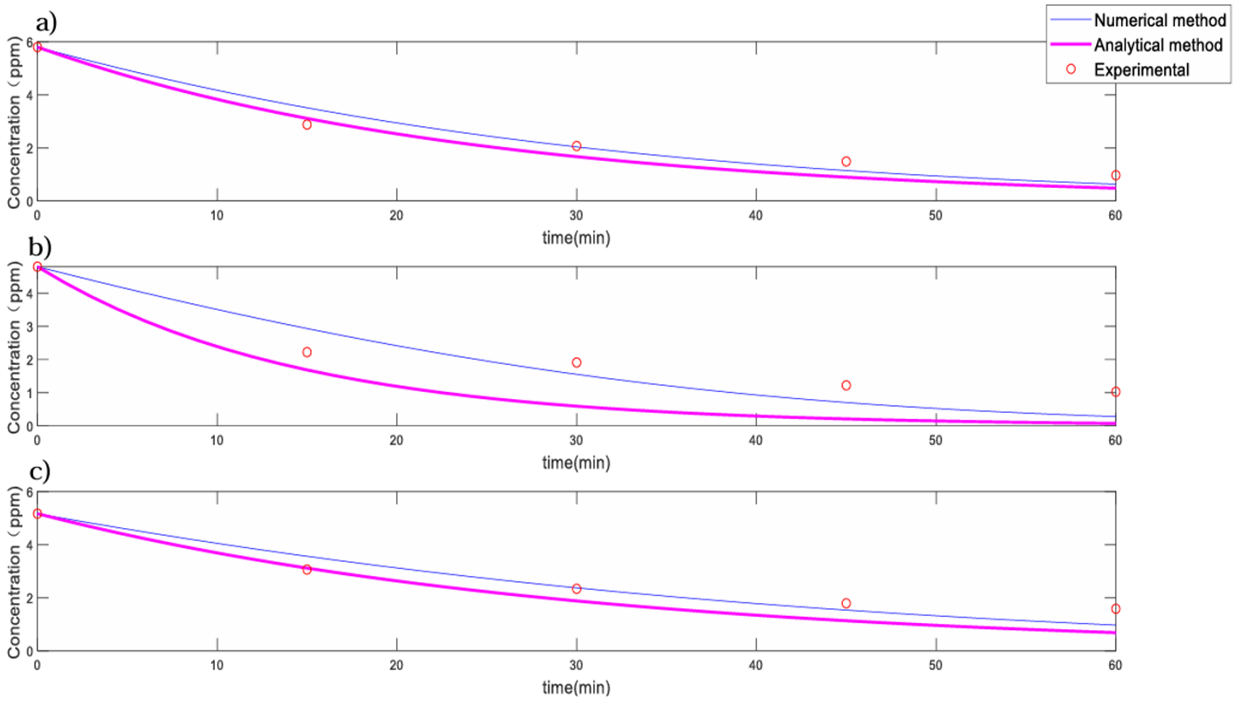

Figure 22. MB concentration (mg/L) versus time for 20 ppm Ag/TiO_2 catalyst in pH of: a) 5; b) 7; c)9.

Experimentally, Ag/TiO_2 has the highest degradation efficiency when the concentration of Ag metal solution is 50 ppm under pH of 5. A model is generated to compare with the experimental model. The result is shown in Figure 25. As can be seen, the model overpredicts the experimental model. At 60 mins UV irradiation, the PE is predicted to be 96.35%, while experimentally it can only reach 83.82 %, but the micro kinetics investigations, as simulated by the LH Model, revealed the applicability of this model to the experimental data. The deviation was possibly caused by experimental error during preparation of MB or Ag/TiO_2 catalyst, The error might impose contamination into the solutions and retard the PE.

Based on experimental observations and kinetic analysis, the degradation of methylene blue (MB) using Ag/TiO_2 can be explained through a series of reactions (Eqs. 1-6). Initially, MB molecules are adsorbed onto the surface of the Ag/TiO_2 catalyst (Eq. 8). This adsorption is a crucial first step in the photocatalytic degradation process, as described by the Langmuir-Hinshelwood kinetic model, which assumes that the reaction occurs between species adsorbed on the catalyst surface. When the Ag/TiO_2 catalyst is exposed to UV or visible light, it absorbs photons,

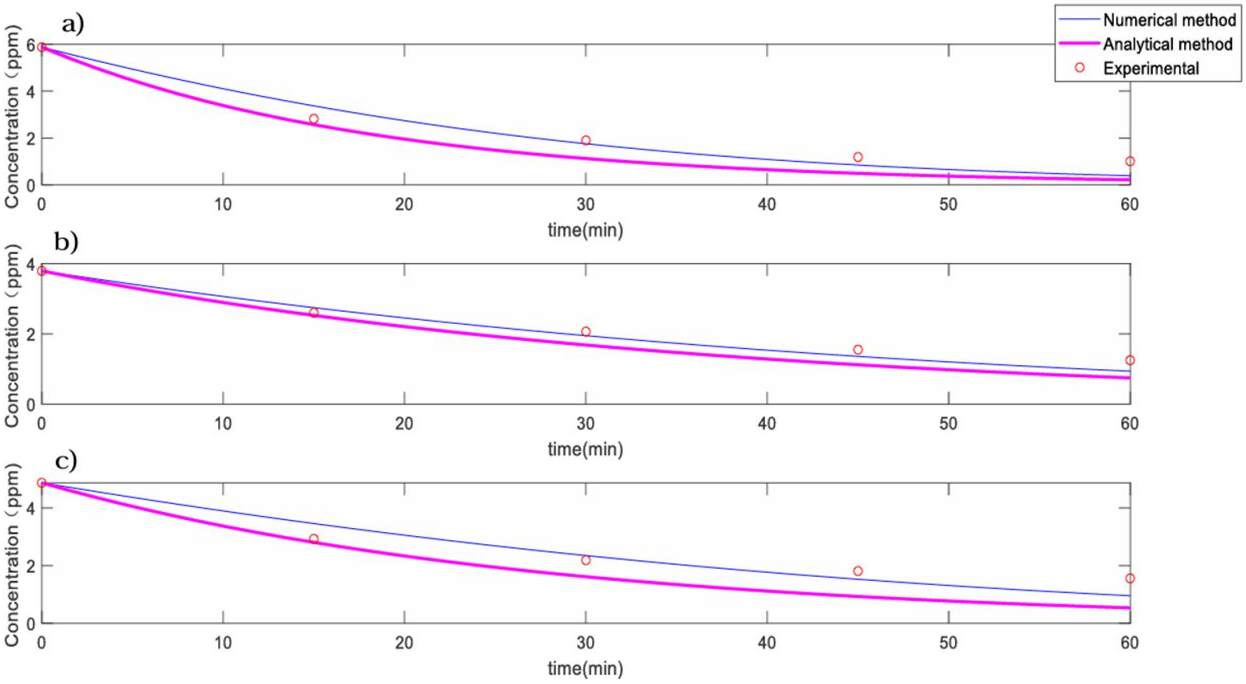

Figure 23. MB concentration (mg/L) versus time for 50 ppm Ag/TiO_2 catalyst in pH: a) 5; b) 7; c) 9.

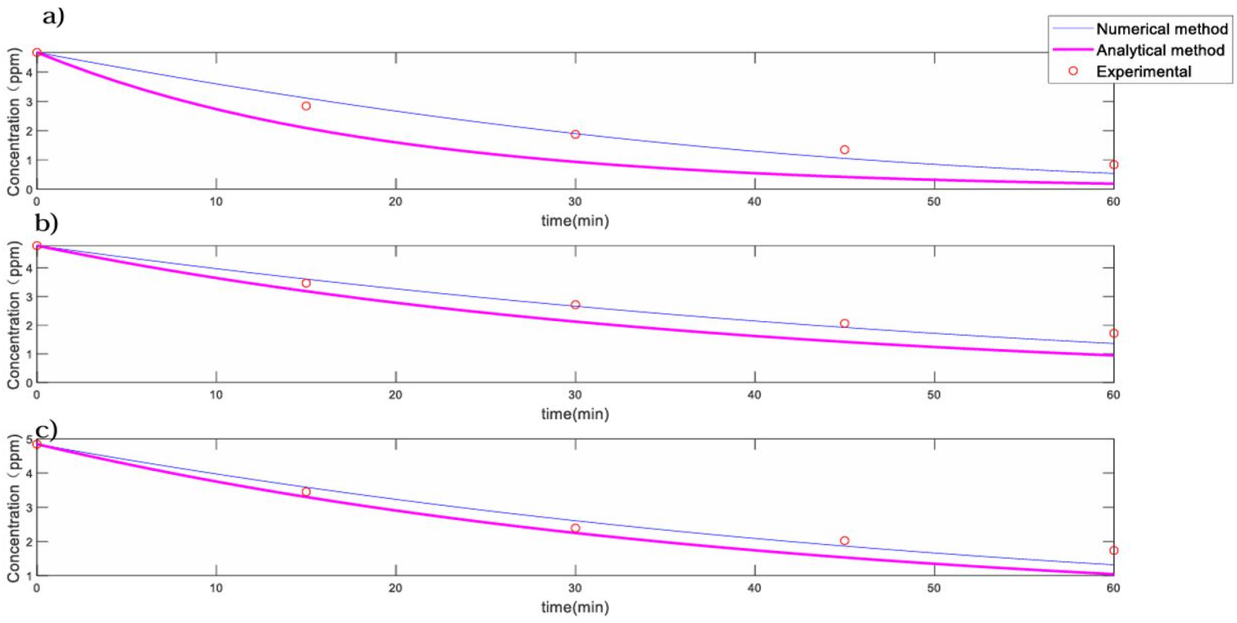

Figure 24. MB concentration (mg/L) versus time for 80 ppm Ag/TiO_2 catalyst in pH: a) 5; b) 7; c) 9.

leading to the formation of electron-hole pairs (Eq. 9). These charge carriers can either recombine and release energy as heat (Eq. 10) or migrate to the catalyst surface, where they initiate redox reactions. Silver plays a significant role in improving photocatalytic efficiency by acting as an electron trap. It captures electrons and thereby reduces the recombination rate of electron-hole pairs, which enhances charge separation and promotes the formation of reactive species.

The photogenerated holes (h^+) can oxidize water molecules or hydroxide ions (OH^-) on the catalyst surface, producing hydroxyl radicals ($\cdot OH$), which are highly reactive and capable of oxidizing organic pollutants (Eqs. 11 and 12). At the same time, the photogenerated electrons (e^-) reduce molecular oxygen adsorbed on the surface to form superoxide radicals ($\cdot O_2^-$) as shown in Eq. 13. These reactive oxygen species (ROS), particularly $\cdot OH$ and $\cdot O_2^-$, attack and degrade MB molecules (Eq. 14). The degradation proceeds through several intermediate steps, eventually leading to harmless end products such as carbon dioxide (CO_2), water (H_2O), protons (H^+), nitrate (NO_3^-), and sulfate ions (SO_4^{2-}), depending on the molecular structure of methylene blue.

$$Ag/TiO_2 + MB \rightarrow Ag/TiO_2\text{-}MB_{Ads.} \quad (8)$$

$$Ag/TiO_2 + hv \rightarrow e^-_{CB} + h^+_{VB} \quad (9)$$

$$e^- + h^+ \rightarrow Heat \quad (10)$$

$$h^+_{VB} + H_2O \rightarrow \cdot OH + H^+ \quad (11)$$

$$h^+_{VB} + OH^- \rightarrow \cdot OH \quad (12)$$

$$e^-_{CB} + O_2 \rightarrow \cdot O_2^- \quad (13)$$

$$\cdot OH/\cdot O_2^- + MB \rightarrow products\ (CO_2, H_2O, H^+, NO_3^-, SO_4^{-2}) \quad (14)$$

4. Conclusion

In this research, Ag/TiO_2 catalyst was successfully synthesized through the liquid impregnation method by using different concentrations of $AgNO_3$ precursor. The element and morphology of Ag/TiO_2 catalyst was confirmed by various characterization techniques like XRD, FESEM, and EDX. Besides, the FTIR confirmed the functional group present in Ag/TiO_2 catalyst. Meanwhile, the zeta potential value suggested that Ag/TiO_2 catalyst is negatively charged and able to attract cationic dye for the photodegradation process. Throughout this research, the photocatalytic performances of TiO_2 particles and Ag/TiO_2 catalyst were examined by the degradation of methylene blue dye. From the experiment, Ag/TiO_2 catalyst has the highest photocatalytic performance when the pH was 5 and the concentration of Ag metal solution was 50 ppm under UV irradiation. All the results were then analysed using a statistical approach to obtain an optimal parameter to have the highest photocatalytic performance. Statistically, Ag/TiO_2 catalyst has the highest photocatalytic performance when the pH is 5 and the concentration of Ag metal solution is 22.63 ppm under UV irradiation. Two mathematical models were generated through numerical (MATLAB) and analytical (PIA) methods and matched with the experimental model. The results indicated that both TiO_2 particles and Ag/TiO_2 catalyst showed a first-order kinetic reaction. The photocatalytic activity was successfully described using Power Law kinetic model, which is derived from the Langmuir-Hinshelwood framework.

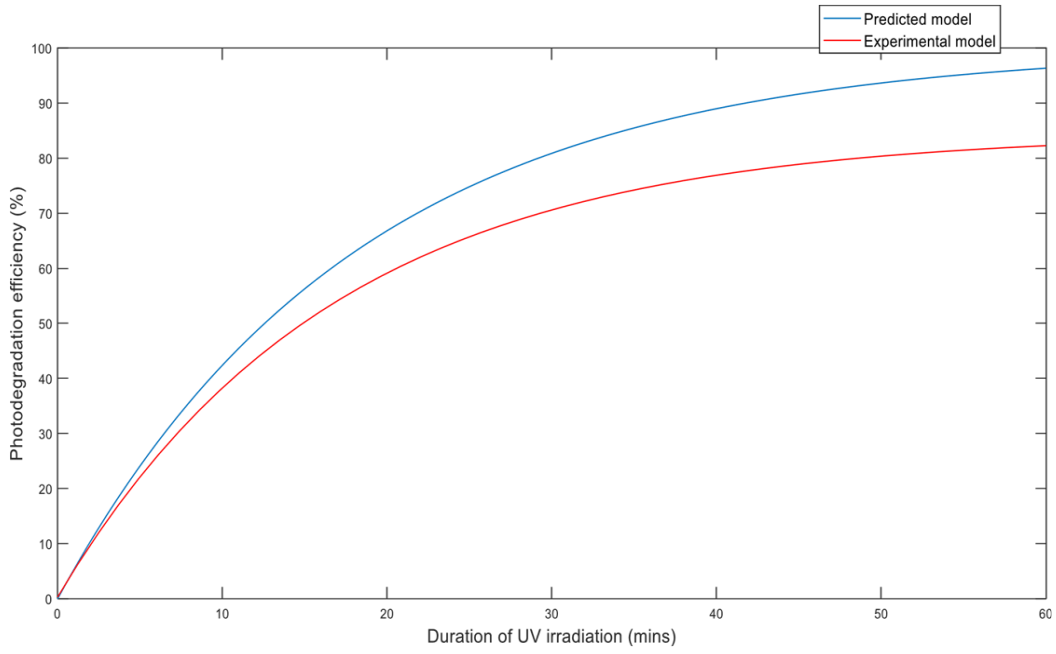

Figure 25. Photodegradation efficiency (%) vs duration of UV irradiation (mins).

Despite some deviation in photodegradation efficiency, the Power Law model effectively represents the experimental data based on microkinetic analysis. Among the modeling approaches applied, the numerical solution method demonstrated better agreement with the experimental data for the photodegradation of methylene blue over Ag/TiO_2 catalysts compared to the analytical method.

Acknowledgments

The authors would like to express their sincere gratitude for the financial support provided by the Ministry of Higher Education Malaysia through the Fundamental Research Grant Scheme (FRGS/1/2022/STG05/USM/03/3). The authors also acknowledge the support received from Universiti Sains Malaysia.

CRedit Author Statement

Author Contributions: Amna Jwad Kadem: Data curation, Formal analysis, Investigation, Methodology, Roles/Writing - original draft. Vengedesweren Durgashene: Data curation, Formal analysis, Investigation, Methodology, Roles/Writing - original draft. Xian Jin Lau: Conceptualization, Formal analysis, Investigation, Methodology, Swee-Yong Pung: Conceptualization, Formal analysis, Funding acquisition, Resources, Validation, Writing - review & editing. Srimala Sreekantan: Conceptualization, Funding acquisition, Resources, Validation, Writing - review & editing. Ramakrishnan Sivakumar: Conceptualization, Formal analysis, Investigation, Project administration, Resources, Supervision, Validation, Writing - review & editing. All authors have read and agreed to the published version of the manuscript.

References

[1] Kapdan, I.K., Kargi, F. (2002). Simultaneous biodegradation and adsorption of textile dyestuff in an activated sludge unit. *Process Biochemistry,* 37 (9), 973–981. DOI: 10.1016/S0032-9592(01)00309-0

[2] Kadirvelu, K., Kavipriya, M., Karthika, C., Radhika, M., Vennilamani, N., Pattabhi, S. (2003). Utilization of various agricultural wastes for activated carbon preparation and application for the removal of dyes and metal ions from aqueous solutions. *Bioresource Technology,* 87(1), 129–132. DOI: 10.1016/S0960-8524(02)00201-8

[3] Riente, P., Noël, T. (2019). Application of metal oxide semiconductors in light-driven organic transformations. *Catalysis Science & Technology,* 9(19), 5186–5232. DOI: 10.1039/c9cy01170f

[4] Han, M., Zhu, S., Lu, S., Song, Y., Feng, T., Tao, S., Liu, J., Yang, B. (2018). Recent progress on the photocatalysis of carbon dots: Classification, mechanism and applications. *Nano Today,* 19, 201–218. DOI: 10.1016/j.nantod.2018.02.008

[5] Zhang, W., Zhang, S., Wang, J., Wang, M., He, Q., Song, J., Wang, H., Zhou, J. (2018). Hybrid functionalized chitosan-Al_2O_3@SiO_2 composite for enhanced Cr(VI) adsorption. *Chemosphere,* 203, 188–198. DOI: 10.1016/j.chemosphere.2018.03.188

[6] Diaz-Angulo, J., Gomez-Bonilla, I., Jimenez-Tohapanta, C., Mueses, M., Pinzon, M., Machuca-Martinez, F. (2019). Visible-light activation of TiO2 by dye-sensitization for degradation of pharmaceutical compounds. *Photochemical & Photobiological Sciences,* 18(4), 897–904. DOI: 10.1039/c8pp00270c

[7] Chong, M.N., Jin, B., Chow, C.W.K., Saint, C. (2010). Recent developments in photocatalytic water treatment technology: A review. *Water Research,* 44(10), 2997–3027. DOI: 10.1016/j.watres.2010.02.039

[8] Sébastien, S. (2012). Les soignants face à la mort. *Revue Infirmière,* 1(180), 39–41.

[9] Yaqoob, A.A., Parveen, T., Umar, K., Mohamad Ibrahim, M.N. (2020). Role of nanomaterials in the treatment of wastewater: A review. *Water,* 12(2), 495. DOI: 10.3390/w12020495

[10] Chauke, N.M., Ngqalakwezi, A., Raphulu, M. (2025). Transformative advancements in visible-light-activated titanium dioxide for industrial wastewater remediation. *International Journal of Environmental Science and Technology,* 22, 8521–8552. DOI: 10.1007/s13762-025-06397-2

[11] Lee, S.-Y., Park, S.-J. (2013). TiO_2 photocatalyst for water treatment applications. *Journal of* Industrial and Engineering Chemistry, 19(6), 1761–1769. DOI: 10.1016/j.jiec.2013.07.012

[12] Huang, Z., Gao, Z., Gao, S., Wang, Q., Wang, Z., Huang, B., Dai, Y. (2017). Facile synthesis of S-doped reduced TiO_2-x with enhanced visible-light photocatalytic performance. *Chinese Journal of Catalysis,* 38(5), 821–830. DOI: 10.1016/S1872-2067(17)62825-0

[13] Micheal, K., Ayeshamariam, A., Boddula, R., Arunachalam, P., Al-Salhi, M.S., Theerthagiri, J., Prasad, S., Madhavan, J., Al-Mayouf, A.M. (2019). Assembled composite of hematite iron oxide on sponge-like BiOCl with enhanced photocatalytic activity. *Materials Science in Energy Technology,* 2(1), 104–111. DOI: 10.1016/j.mset.2018.11.004

[14] Yin, S., Zhang, Q., Saito, F., Sato, T. (2003). Preparation of visible light-activated titania photocatalyst by mechanochemical method. *Chemistry Letters,* 32(4), 358–359. DOI: 10.1246/cl.2003.358

[15] Moma, J., Baloyi, J. (2019). Modified Titanium Dioxide for Photocatalytic Applications. *Photocatalysts - Applications and Attributes* (p. 18). DOI: 10.5772/intechopen.79374

[16] Widiyandari, H., Nashir, M., Parasdila, H., Almas, K.F., Suryana, R. (2023). Ag-TiO_2 for efficient methylene blue photodegradation under visible light irradiation. *Bulletin of Chemical Reaction Engineering & Catalysis,* 18(4), 593–603. DOI: 10.9767/bcrec.19885

[17] Feng, S., Wang, M., Zhou, Y., Li, P., Tu, W., Zou, Z. (2015). Double-shelled plasmonic Ag-TiO_2 hollow spheres toward visible-light-active photocatalytic conversion of CO_2 into solar fuel. *APL Materials,* 3(10), 104416. DOI: 10.1063/1.4930043

[18] Cai, P.-F., Li, J., Wu, X.-B., Li, Z.-Y., Shen, J., Nie, J.-J., Cui, Z.-D., Chen, D.-F., Liang, Y.-Q., Zhu, S.-L., Wu, S.-L. (2022). ALD-induced TiO_2/Ag nanofilm for rapid surface photodynamic ion sterilization. *Rare Metals,* 41(12), 4138–4148. DOI: 10.1007/s12598-022-02096-w

[19] Jarandehei, A., Golpayegani, M.K., De Visscher, A. (2008). Kinetic modeling of photocatalytic degradation reactions: Effect of charge trapping. *Applied Catalysis B: Environmental,* 84(1–2), 65–74. DOI: 10.1016/j.apcatb.2008.03.006

[20] Kumar, K.V., Porkodi, K., Rocha, F. (2008). Langmuir Hinshelwood kinetics – A theoretical study. *Catalysis Communications,* 9(1), 82–84. DOI: 10.1016/j.catcom.2007.05.019

[21] Chen, W.-T., Chan, A., Sun-Waterhouse, D., Llorca, J., Idriss, H., Waterhouse, G.I.N. (2018). Performance comparison of Ni/TiO_2 and Au/TiO_2 photocatalysts for H_2 production in different alcohol–water mixtures. *Journal of Catalysis,* 367, 27–42. DOI: 10.1016/j.jcat.2018.08.015

[22] Kim, M.G., Kang, J.M., Lee, J.E., Kim, K.S., Kim, K.H., Cho, M., Lee, S.G. (2021). Effects of calcination temperature on the phase composition, photocatalytic degradation, and virucidal activities of TiO_2 nanoparticles. *ACS Omega,* 6(16), 10668-10678. DOI: 10.1021/acsomega.1c00043

[23] Komaraiah, D., Radha, E., Sivakumar, J., Ramana Reddy, M.V., Sayanna, R. (2020). Photoluminescence and photocatalytic activity of spin-coated Ag^+-doped anatase TiO_2 thin films. *Optical Materials,* 108, 110401. DOI: 10.1016/j.optmat.2020.110401

[24] Wang, W., Serp, P., Kalck, P., Faria, J.L. (2005). Photocatalytic degradation of phenol on MWNT and titania composite catalysts prepared by a modified sol-gel method. *Applied Catalysis B: Environmental,* 56(4), 305–312. DOI: 10.1016/j.apcatb.2004.10.036

[25] Kumar, R., Rashid, J., Barakat, M.A. (2015). Zero valent Ag deposited TiO_2 for the efficient photocatalysis of methylene blue under UV-C light irradiation. *Colloids and Interface Science Communications,* 5, 1–4. DOI: 10.1016/j.colcom.2015.05.001

[26] Padmanaban, A., Dhanasekaran, T., Kumar, S. P., Gnanamoorthy, G., Munusamy, S., Stephen, A., Narayanan, V. (2017). Visible light photocatalytic property of Ag/TiO_2 composite. *Mechanics, Materials Science & Engineering Journal*, 9(1). DOI: 10.2412/mmse.97.67.748

[27] Pelaez, M., Nolan, N.T., Pillai, S.C., Seery, M.K., Falaras, P., Kontos, A.G., Dunlop, P.S.M., Hamilton, J.W.J., Byrne, J.A., O'Shea, K., Entezari, M.H., Dionysiou, D.D. (2012). A review on the visible light active titanium dioxide photocatalysts for environmental applications. *Applied Catalysis B: Environmental*, 125, 331–349. DOI: 10.1016/j.apcatb.2012.05.036

[28] Kadem, A.J., Teo, Y.X., Pung, S., Sreekantan, S., Ramakrishnan, S. (2023). Predicting photocatalytic properties of metal coupled Mn-TiO_2 particle using response surface methodology (RSM) as a potential filler in LED's encapsulant. *Bulletin of Chemical Reaction Engineering & Catalysis,* 18(2), 238-255. DOI: 10.9767/bcrec.18020

[29] Chakhtouna, H., Benzeid, H., Zari, N., Qaiss, A.E.K., Bouhfid, R. (2021). Recent progress on Ag/TiO_2 photocatalysts: Photocatalytic and bactericidal behaviors. *Environmental Science and Pollution Research,* 28(33), 44638–44666. DOI: 10.1007/s11356-021-14996-y

[30] Jodat, A., Jodat, A. (2014). Photocatalytic degradation of chloramphenicol and tartrazine using Ag/TiO_2 nanoparticles. *Desalination and Water Treatment,* 52(13–15), 2668–2677. DOI: 10.1080/19443994.2013.794115

[31] Jiang, D., Kusdianto, K., Kubo, M., Shimada, M. (2020). Effect of Ag loading content on morphology and photocatalytic activity of Ag-TiO_2 nanoparticulate films prepared via simultaneous plasma-enhanced chemical and physical vapor deposition. *Materials Research Express,* 7(11), 116406. DOI: 10.1088/2053-1591/abc720

[32] Kulkarni, R.M., Malladi, R.S., Hanagadakar, M.S., Doddamani, M.R., Bhat, U.K. (2016). Ag-TiO_2 nanoparticles for photocatalytic degradation of lomefloxacin. *Desalination and Water Treatment*, 57(34), 16111-16118. DOI: 10.1080/19443994.2015.1076352

[33] Lantos, E., Mérai, L., Deák, Á., Gómez-Pérez, J., Sebők, D., Dékány, I., Kónya, Z., Janovák, L. (2020). Preparation of sulfur hydrophobized plasmonic photocatalyst towards durable superhydrophobic coating material. *Journal of Materials Science & Technology*, 41, 159-167. DOI: 10.1016/j.jmst.2019.04.046

[34] Tang, J., Zou, Z., Ye, J. (2005). Kinetics of MB degradation and effect of pH on the photocatalytic activity of MIn_2O_4 (M= Ca, Sr, Ba) under visible light irradiation. *Research on chemical intermediates*, 31(4), 513-519. DOI: 10.1163/1568567053956699

[35] Saeed, M., Muneer, M., Khosa, M., Akram, N., Khalid, S., Adeel, M., Nisar, A. Sherazi, S. (2019). Azadirachta indica leaves extract assisted green synthesis of Ag-TiO_2 for degradation of Methylene blue and Rhodamine B dyes in aqueous medium. *Green Processing and Synthesis,* 8(1), 659-666. DOI: 10.1515/gps-2019-0036

[36] Schneider, J., Matsuoka, M., Takeuchi, M., Zhang, J., Horiuchi, Y., Anpo, M., Bahnemann, D.W. (2014). Understanding TiO_2 photocatalysis: Mechanisms and materials. *Chemical Reviews,* 114(19), 9919–9986. DOI: 10.1021/cr5001892

[37] Khataee, A.R., Kasiri, M.B. (2010). Photocatalytic degradation of organic dyes in the presence of nanostructured titanium dioxide: Influence of the chemical structure of dyes. *Journal of Molecular Catalysis A: Chemical*, 328(1-2), 8-26. DOI: 10.1016/j.molcata.2010.05.023

[38] Le, A.T., Pung, S.Y., Chiam, S.L., Josoh, N.B.N., Koay, T.Y., Lee, J.S., Mustar, N.B. (2020, September). Photocatalytic performance of TiO_2 particles in degradation of various organic dyes under visible and UV light irradiation. In *AIP Conference Proceedings* (Vol. 2267, No. 1, p. 020017). AIP Publishing LLC. DOI: 10.1063/5.0016025